International Journal of Control and Automation
Vol. 7, No. 12 (2014), pp. 199-218
http://dx.doi.org/10.14257/ijca.2014.7.12.19

An Artificial Intelligence Based System Identification of AC-DC Power System Including a Three-Phase Controlled Rectifier

Peera Ruttanee, Kongpan Areerak and Kongpol Areerak

School of Electrical Engineering, Institute of Engineering
Suranaree University of Technology
Nakhon Ratchasima 30000, Thailand
Corresponding Author e-mail: kongpan@sut.ac.th
Tel: +66-44224520; Fax: +66-44224601

Abstract

The artificial intelligence techniques are widely applied to many works of engineering. This paper presents the application of the artificial intelligence techniques to identify the AC-DC power system parameters. The DC-link filters are normally included in such power systems. For some applications, accurate DC-link filter parameters are very important for the system analysis and design. According to the measurement errors and a large variation in a capacitor value, the parameter identification is needed to provide the accurate parameters. Therefore, the paper presents the identification of DC-link filter parameters using the adaptive tabu search technique and the genetic algorithm. The experimental results from the testing rig and the averaging model of the system are used in the searching process. The identification results show that the accurate DC-link filter parameters including line parameters on the AC side can be easily obtained via the proposed method. Moreover, the resulting parameters are very useful for a stability analysis of the power electronic systems due to a constant power load.

Keywords*: System identification, Artificial Intelligence, AC-DC converter*

1. Introduction

Power electronic converters are widely used in many applications. The AC-DC power system including a three-phase controlled rectifier feeding a constant power load (CPL) is considered in the paper. The CPL can significantly degrade the system stability [1-4]. Therefore, the dynamic model of the power system with CPL is very important for stability studies. It is well known that the accurate mathematical model of the power electronic based system feeding the CPL suitable for the stability analysis can be derived from many averaging techniques [5-12]. Unfortunately, only accurate dynamic model cannot predict the correct unstable point of the practical system because we do not know the accurate system parameters. From the previous works, the DC-link filter parameters are very important for the stability analysis [13-15]. According to the measurement errors and the large variation in the capacitor value, the identification of such parameters is needed to provide the usable parameters. From the previous publications [16-19], the artificial intelligence (AI) techniques can be applied to the system identifications. However, the applications of AI to the system identifications of the power electronic based system have not been reported in the previous works [16–19]. This is because the objective function of the power electronic system is very complex. In addition, during the identification process via the AI methods, the simulation of the power electronic system is repeated in the objective function. The transient simulations of

ISSN: 2005-4297 IJCA

the power electronic system consume the huge simulation time due to the switching devices in the circuit. Due to the vast simulation time of the switching devices, the application of AI techniques is not widely applied to identify the system parameters of the power electronic based system. Therefore, this paper presents the identification of DC-link filter parameters including line parameters on the AC side of the AC-DC power system with a three-phase controlled rectifier using the AI techniques called the adaptive tabu search (ATS) and genetic algorithm (GA). To solve the simulation time problem, the averaging model of AC-DC power system derived from the DQ method [10-15] can be also used in the paper instead of the exact topology model. This is because the simulation time of the averaging DQ model is faster than that from the full switching model. The resulting DQ model is used as the objective function for the searching process of ATS and GA. The experimental results from the testing rig are also used in the searching process to ensure that the accurate system parameters can be achieved. The identification results show that the accurate DC-link filter parameters including line parameters on the AC side can be easily obtained via the proposed method. Moreover, the resulting parameters are very useful for a stability analysis of the power electronic systems due to a CPL. Although the system parameters identified from ATS and GA algorithms are not the same, the use of dynamic model with these different parameters can provide the same unstable point.

The paper is structured as follows. In Section 2, the considered power system is illustrated. In Section 3, the testing rig that we need to identify the system parameters is addressed. The ATS and GA algorithms are briefly explained in Section 4. In Section 5, the system identification of the testing system using the proposed method is fully shown. In addition, the application of the system parameters identified by the proposed technique to stability studies is illustrated in Section 6. Finally, Section 7 concludes and discusses the advantages of the proposed technique for the system identification of the power electronic systems.

2. The Considered Power System

The power system studied in this paper is depicted in Figure 1. It consists of a three-phase voltage source, transmission line, three-phase controlled rectifier, DC-link filters, and an ideal CPL connected to the DC bus. The ideal CPL is used to represent actuator drive systems by assuming an infinitely fast controller action of the drive system. Hence, the ideal CPL can be considered as a voltage-dependent current source given by (1).

$$I_{CPL} = \frac{P_{CPL}}{U_{dc}} \tag{1}$$

where U_{dc} is the voltage across the CPL and P_{CPL} is the power level of CPL.

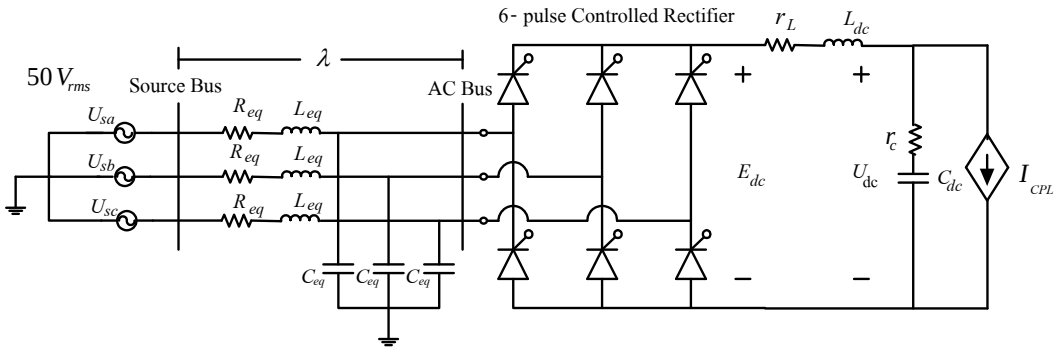

Figure 1. The considered AC-DC power system

From the previous researches [1-4], the CPL can significantly degrade the system stability. Hence, in this paper, the unstable point of the studied power system in Figure 1 will be predicted via the reported dynamic model [20]. However, the aim of the paper is to identify the system parameters that are usable for the stability study. The details how to use the ATS and GA algorithms for the system identification will be explained in Section 5.

3. The Testing System

As mentioned in Section 1, the accurate system parameters of the system in Figure 1 are very important for stability studies, especially R_{eq}, L_{eq}, r_L, L_{dc}, r_c, and C_{dc}. In Figure 1, the ideal CPL does not affect the values of these parameters. Hence, the CPL is replaced by the R_{test} as shown in Figure 2 in which this figure is the testing system for the system identification. When R_{eq}, L_{eq}, r_L, L_{dc}, r_c, and C_{dc} are already determined by using the proposed technique, the dynamic model of the system in Figure 1 with the identified parameters will be used for the stability analysis.

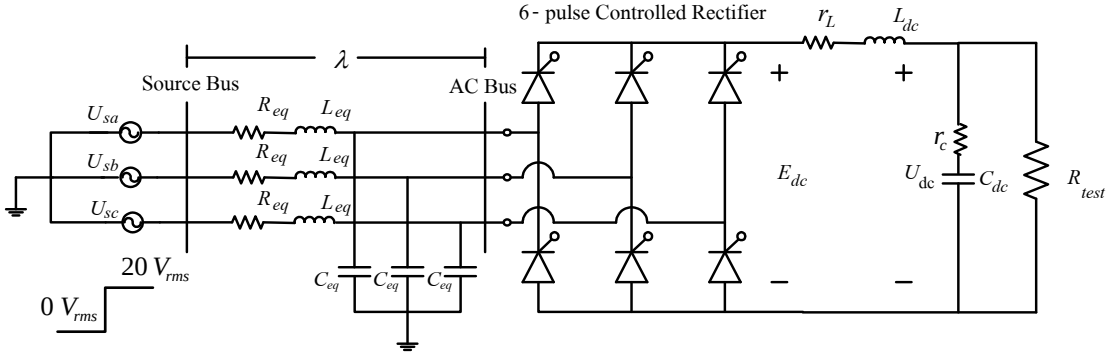

Figure 2. The Diagram of the Damping Test System

The resistance and inductance of the DC-link filter can be easily measured from the LCR meter. The three-phase line capacitances are very small. They can be set to 2nF for the mathematical model. This is because the DQ mathematical model for the diode rectifier requires a voltage source which can be provided by these capacitances. The more details of the mathematical model of the system in Figure 1 derived from the DQ method can be found in [20]. For the DC-link capacitance, two capacitors 470 μF in series were used. The variation of the capacitance value for each capacitor is from -10% to 50%, typical of electrolytic capacitors. Therefore, to achieve usable parameter values of capacitance (r_c and C_{dc}), a step response test as shown in Figure 2 was carried out. In addition, the AC line parameters R_{eq} and L_{eq} can be determined via this step response test as well. A step change of the voltage source from 0 V_{rms} to 20 V_{rms} with the different firing angle of the thyrister (α) was used to achieve the transient output voltage responses. These responses will be later used in the system identification using the ATS and GA methods. The testing rig of the damping test is depicted in Figure 3. The results from the testing rig in Figure 3 will be called $U_{dc(experiment)}$ that will be used in the ATS and GA searching processes.

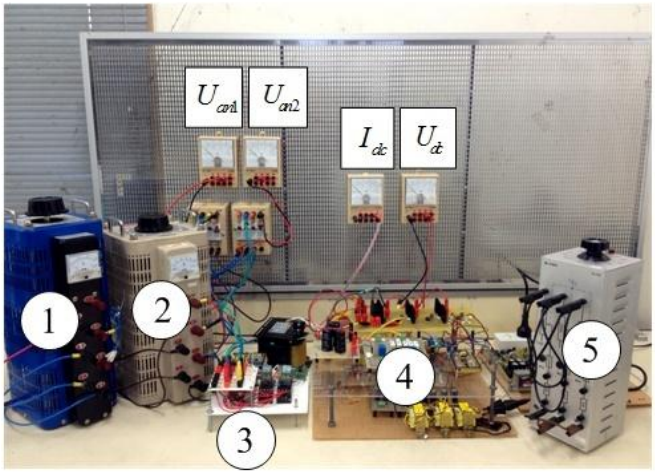

1. Three-Phase Voltage Source 1
2. Three-Phase Voltage Source 2
3. 3-Pole Input Switch
4. Three-Phase Controlled Rectifier
5. Resistance 300 W for Three-Phase Controlled Rectifier

Figure 3. The Rig of the Damping Test System

In this paper, the transient responses from the rig were used to determine the parameter values of DC-link capacitance (r_c and C_{dc}) and the AC line parameters (R_{eq} and L_{eq}) by using the ATS and GA methods. For r_L and L_{dc}, these parameters were determined from the measurement by using a LCR meter. The r_L and L_{dc} of the testing rig in Fig. 3 are equal to 0.57 Ω and 37.7 mH, respectively.

4. The Reviews of ATS and GA Algorithms

In this section, the ATS and GA algorithms are briefly explained.

A. The ATS Algorithm

The ATS algorithm is improved from the Tabu Search (TS) method by adding two mechanisms namely back-tracking and adaptive search radius. The modified version of the TS method has been named the adaptive tabu search of ATS. The ATS algorithm can be outlined as follows:

Step 1: Initialize the tabu list *TL*, and *Count* (a number of search round) = 0.

Step 2: Randomly select the initial solution S_0 from the search space. S_0 is set as a local minimum and S_0 = *best_neighbor* as shown in Figure 4.

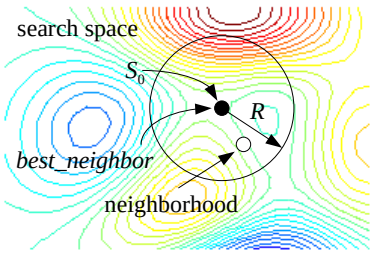

Figure 4. Random S0 in Search Space

Step 3: Update *Count*, then randomly select *N* new solutions from the search space of a radius *R*. Let $S_1(r)$ be a set containing *N* solutions as shown in Figure 5

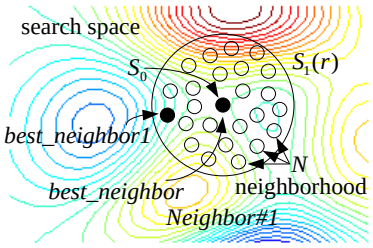

Figure 5. Neighborhood Around S0

Step 4: Compute the cost value of each member of $S_1(r)$. Then, choose the best solution and assign it as *best_neighbor1* (see Figure 5).
Step 5: If *best_neighbor1* < *best_neighbor*, then keep *best_neighbor* in the *TL*, set *best_neighbor* = *best_neighbor1* (see Figure 6), and set S_0 = *best_neighbor* (see Figure 7). Otherwise, put *best_neighbor1* in the *TL* instead.

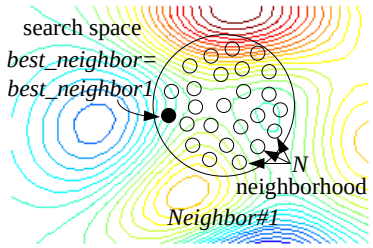

Figure 6. Assign a New Best_neighbor

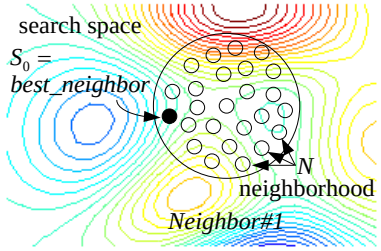

Figure 7. Assign a New S0

Step 6: Evaluate the termination criteria (*TC*) and the aspiration criteria (*AC*). If *Count* ≥ *MAX_Count* (the maximum number allowance of search round), stop the searching process. The current best solution is the overall best solution. Otherwise, go back to Step 2 and start the searching process again until all criteria is satisfied (see Figure 8).

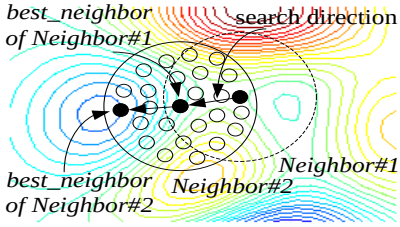

Figure 8. Searching Process in the Next Iteration

The back-tracking process allows the system to go back and look up the previous solutions in *TL*. The better solution is then chosen among the current and the previous solutions. Figure 9 illustrates details of the back-tracking process.

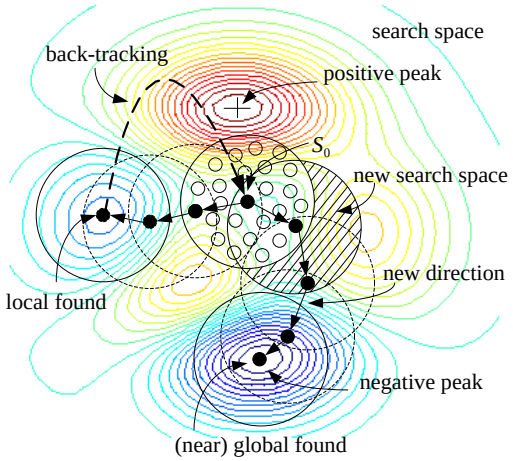

Figure 9. Back-tracking in ATS Algorithm

Given this new search space to explore, the search process is likely to have more chances of escaping from the local optimum. The back-tracking mechanism can be added into Step 5 to improve the searching performance.

The adaptive radius process as depicted in Fig. 10 decreases the search area during the searching process. The adaptive radius mechanism has been developed to adjust the radius (*R*) by using the cost of the solution. The criterion for adapting the search radius is given in (2).

$$radius_{new} = \frac{radius_{old}}{DF} \tag{2}$$

where *DF* is a decreasing factor. The adaptive search radius mechanism can be added into the end of Step 6 to improve the searching performance. The more details of ATS algorithm can be found in [16-19].

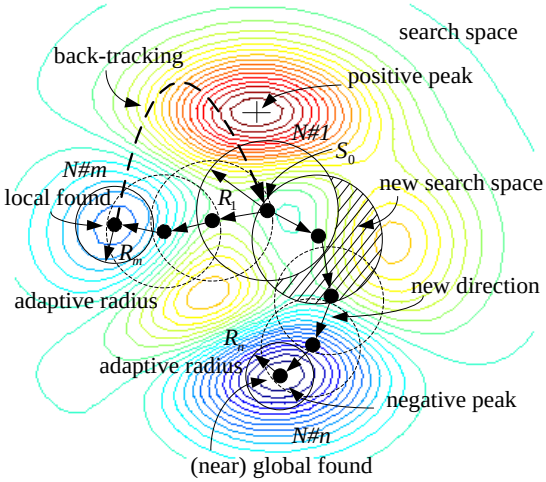

Figure 10. ATS Algorithm with Adaptive Search Radius Mechanism

B. The GA Algorithm

The summarized GA algorithm is given in Figure 11.

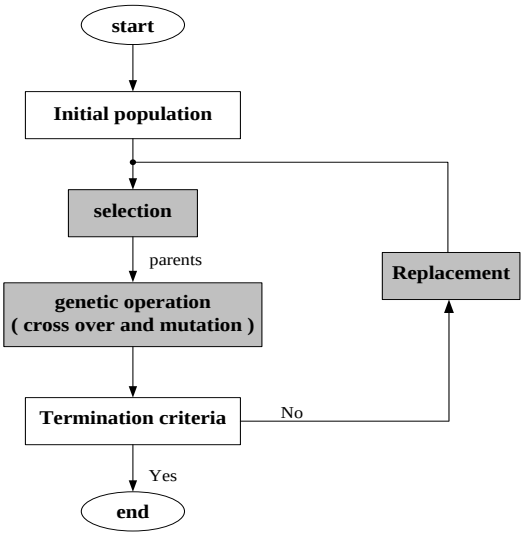

Figure 11. The Process of GA Algorithm

Figure 11 shows the three main processes for the GA method that are *selection*, *genetic operation*, and *replacement*. According to the Figure 11, the steps of the GA approach are summarized as follows:
Step 1: Generate randomly population of x chromosomes as the initial population.
Step 2: Evaluate the fitness $f(x)$ of each chromosome x in the population.
Step 3: Create a new population by using the following three main processes:
Selection: This process will select the chromosomes in the population to be the parents for the next generation. The selection criteria is based on their fitness values in which the chromosome providing the better fitness will has the bigger opportunity to be selected.
Genetic operation: This process will create a new offspring from the parents by using the crossover and mutation probabilities.
Replacement: The offspring from the genetic operation will replace into the previous population in which it may replace the whole of population or some part of population depending on the conditions in the algorithm.
Step 4: If the stop condition is satisfied, stop the searching process. The current best solution is the overall best solution. Otherwise, go back to Step 2 and start the searching process again until all criteria is satisfied.

5. System Identification Using ATS and GA Methods

In Section 4, the ATS and GA algorithms are briefly explained. In this section, the ATS and GA methods are applied to determine the parameters of the proposed system. The block diagram to describe how to use ATS and GA searching methods to identify the system parameters is shown in Figure 12. The experimental results for a step change of the voltage source from 0 V_{rms} to 20 V_{rms} with α equal to 0, 10, and 20 degrees is applied in the searching process, while the results for α equal to 30 degrees will be used for validation. Note that the initial values of C_{dc} and r_c are defined from the measurement.

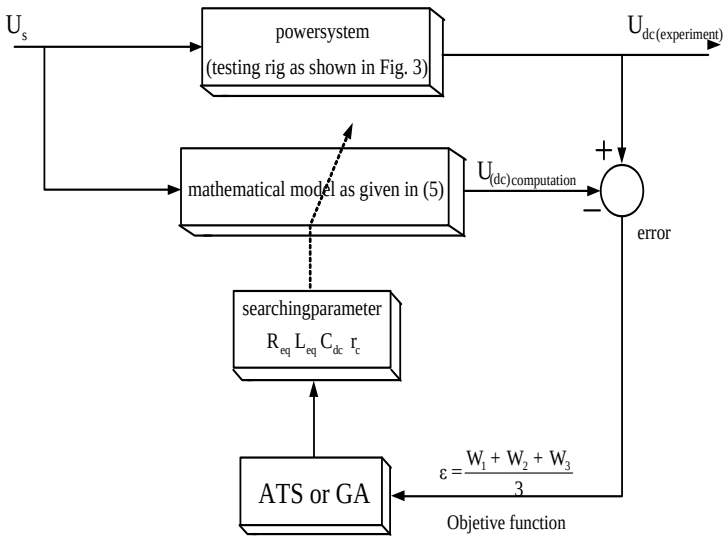

Figure 12. The Applications of ATS and GA Algorithms to the System Identification

As can be seen in Figure 12, the ATS and GA will search the system parameters here are R_{eq}, L_{eq}, r_c and C_{dc}. Then, these parameters from the ATS and GA searching processes are used with the mathematical model derived from the DQ method to calculate the transient output voltage response when a step change of the voltage source U_s from 0 V_{rms} to 20 V_{rms} with α equal to 0, 10 , and 20 degrees is applied. The transient output voltage response calculated from the DQ model with parameters from the ATS and GA methods is called $U_{dc(computation)}$ as shown in Figure 12. The transient output voltage with the same input condition from the testing rig (experiment) as shown in Figure 3 of Section 3 is called $U_{dc(experiment)}$. The system parameters in the model are varied following on the ATS and GA algorithms as explained in Section 4 until a matched voltage response between $U_{dc(computation)}$ and $U_{dc(experiment)}$ is obtained.

In terms of an optimization problem, the ATS and GA will search the appropriate system parameters to minimize the error value (W) between the simulation and the experiment. This error can be calculated by using the definition as given in (3).

$$W_x = \sqrt{\frac{\sum error^2}{n}} \tag{3}$$

where *error* is equal to $\left|U_{dc(computation)} - U_{dc(experiment)}\right|$, n is the number of data used for both testing and calculation, and x equals to 1, 2, and 3 for the data of the system with α equal to 0, 10, and 20, respectively. For this paper, the single objective (*SO*) is used in the searching process. Therefore, the *SO* function is the average value of W_1, W_2, and W_3 as given in (4).

$$\varepsilon = \sum_{x=1}^{\beta} \frac{W_x}{\beta} \tag{4}$$

where β is the number of the data used in the searching process in which it is equal to 3 in the paper because we use the experimental results for a step change of the voltage source from 0 V_{rms} to 20 V_{rms} with α equal to 0, 10, and 20 degrees (3 sets of the data). Therefore, the ATS and GA algorithms will tune the system parameters until the minimum value of ε is obtained.

In Figure 12, the mathematical model of the testing system in Figure 2 is needed to provide the $U_{dc(computation)}$. In this paper, the averaging model derived from the DQ method is selected instead of the full switching model. This is because the simulation of the system in Figure 2 by using the full switching model of software package requires the huge simulation time. According to the vast simulation time, the exact topology model is not suitable for the system identification using the searching method. Therefore, the averaging model required the fast simulation time is selected to provide the transient output voltage response.

The DQ method is used to derive the dynamic model of the testing system in Figure 2 in which the three-phase controlled rectifier can be treated as a transformer. As a result, the equivalent circuit of the power system of Figure 2 can be represented in the DQ frame as depicted in Figure 13.

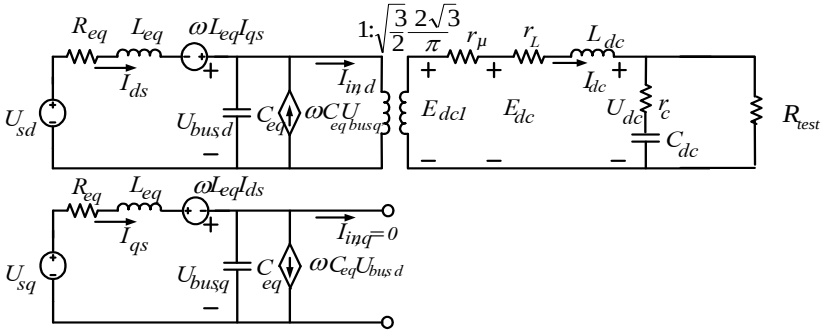

Figure 13. The Equivalent Circuit of the Damping Test System on DQ Frame

The DQ method is selected to eliminate the switching action to achieve the averaging model in which the fast simulation time can be obtained. Applying the KVL and KCL into the circuit of Figure 13, the dynamic model of the damping test system can be expressed as given in (5). The λ in (5) can be calculated by using the power flow equation. The more details how to derive the dynamic model in (5) with calculation of λ in the model can be found in [20].

$$\begin{cases} \dot{I}_{ds} = -\dfrac{R_{eq}}{L_{eq}} I_{ds} + \omega I_{qs} - \dfrac{1}{L_{eq}} U_{bus,d} + \dfrac{1}{L_{eq}} \sqrt{\dfrac{3}{2}} . \dfrac{\cos(\lambda+\alpha)}{L_{eq}} . U_m \\ \dot{I}_{qs} = -\omega I_{ds} - \dfrac{R_{eq}}{L_{eq}} I_{qs} - \dfrac{1}{L_{eq}} U_{bus,q} + \dfrac{1}{L_{eq}} \sqrt{\dfrac{3}{2}} . \dfrac{\sin(\lambda+\alpha)}{L_{eq}} . U_m \\ \dot{U}_{bus,d} = \dfrac{1}{C_{eq}} I_{ds} + \omega U_{bus,q} - \sqrt{\dfrac{3}{2}} \dfrac{2\sqrt{3}}{\pi C_{eq}} I_{dc} \\ \dot{U}_{bus,q} = -\omega U_{bus,d} + \dfrac{1}{C_{eq}} I_{qs} \\ \dot{I}_{dc} = \sqrt{\dfrac{3}{2}} \dfrac{2\sqrt{3}}{\pi L_{dc}} U_{bus,d} - \left(\dfrac{r_L}{L_{dc}} + \dfrac{r_\mu}{L_{dc}} + \dfrac{r_c}{L_{dc}} \right) I_{dc} - \left(\dfrac{R_{test} - r_c}{R_{test} L_{dc}} \right) U_{dc} \\ \dot{U}_{dc} = \dfrac{1}{C_{dc}} I_{dc} - \dfrac{1}{R_{test} C_{dc}} U_{dc} \end{cases} \quad (5)$$

The model in (5) can be coded in MATLAB to provide the output voltage response $U_{dc(computation)}$ with the fast simulation time. This dynamic model is suitable for the ATS and GA searching methods having diagram in Figure 12. The input of the model has to be the

same as that of the testing rig (experiment); here is the step change of the voltage source from 0 V_{rms} to 20 V_{rms} with α equal to 0, 10, and 20 degrees. Then, both transient output voltage responses can be used within the searching process to determine the system parameters.

The searching process was conducted 5 trials with random initial solutions. The proposed method provides the solutions with the averaged value. The identified system parameters from the ATS and GA searching method are given in Table I.

Table 1. The System Parameters Determined from the ATS and GA Methods

ATS Method					
firing angle	$R_{eq}(W)$	$L_{eq}(mH)$	$C_{dc}(mF)$	$r_c(W)$	ε
$a = 0^o$	0.0874	0.12752	234.20	2.992	0.6789
$a = 10^o$	0.0874	0.12752	234.20	2.992	
$a = 20^o$	0.0874	0.12752	234.20	2.992	
GA Method					
$a = 0^o$	0.0062	0.16910	227.95	3.2699	0.64926
$a = 10^o$	0.0062	0.16910	227.95	3.2699	
$a = 20^o$	0.0062	0.16910	227.95	3.2699	

To validate the results in Table I, the damping test system in Figure 2 was simulated with the system parameters as given in Table I including r_L = 0.57 Ω and L_{dc} = 37.7 mH (from measurement) for the step change of the voltage source from 0 V_{rms} to 20 V_{rms} with α equal to 0, 10, and 20 degrees. The comparison results of the output voltage responses from the simulation via the software package (exact topology model) using the parameters identified from the ATS method and experimental results from the testing rig with α equal to 0, 10, and 20 degrees are shown in Figure 14 – Figure 16, respectively.

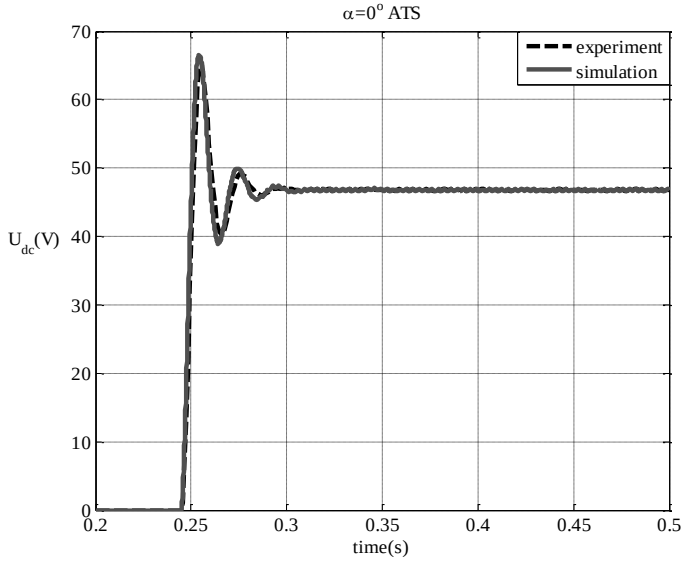

Figure 14. The Comparison Results to Validate the Identified Parameters from the ATS Method (α = 0o)

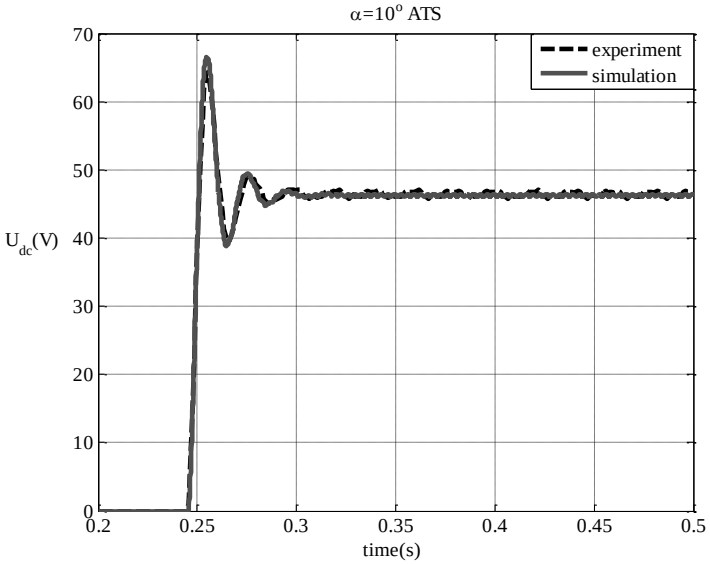

Figure 15. The Comparison Results to Validate the Identified Parameters from the ATS Method (α = 10o)

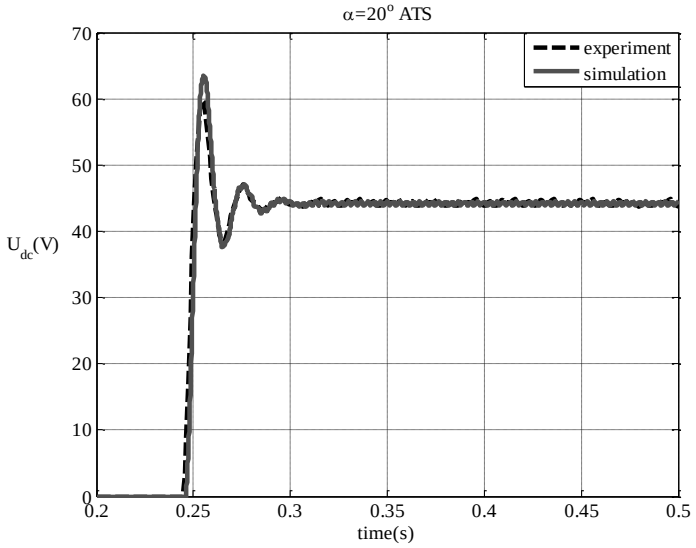

Figure 16. The Comparison Results to Validate the Identified Parameters from the ATS Method (α = 20o)

It can be seen from Figure 14 – Figure 16 that a good agreement of the voltage responses from the model and the experiment is achieved. It means that the accurate parameters of the system can be obtained via the ATS searching method. However, the experimental results with α equal to 0, 10, and 20 degrees were used in the ATS searching process. Hence, in the paper the experimental result with α equal to 30 degrees that was not used in the ATS searching process are compared with the simulation. The comparison result is depicted in Figure 17.

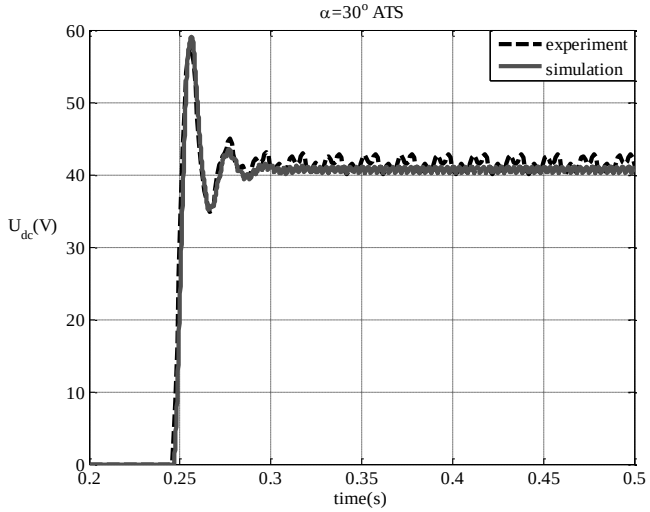

Figure 17. The Comparison Results to Validate the Identified Parameters from the ATS Method (α = 30o)

Although the experimental result with $\alpha = 30^o$ is not used in the ATS searching process, a good agreement between the simulation and the experiment is obtained. This is to confirm that the resulting parameters from the ATS method are accurate.

Similarly, the results from the GA algorithm are given in Figure 18 – Figure 21.

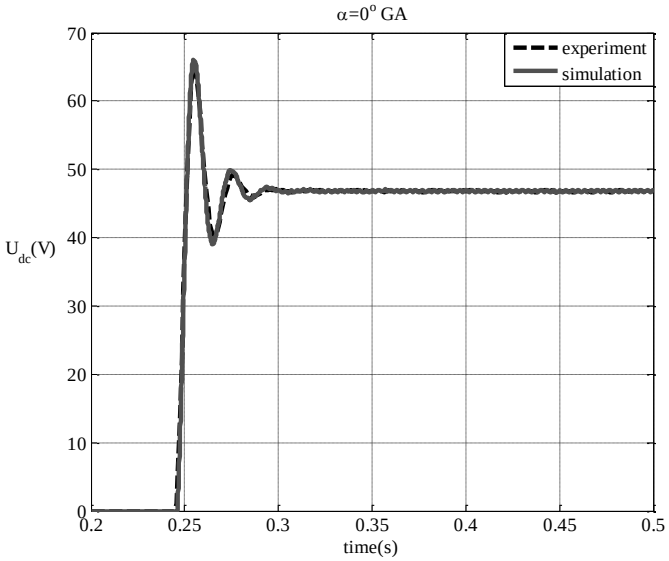

Figure 18. The Comparison Results to Validate the Identified Parameters from the GA Method (α = 0o)

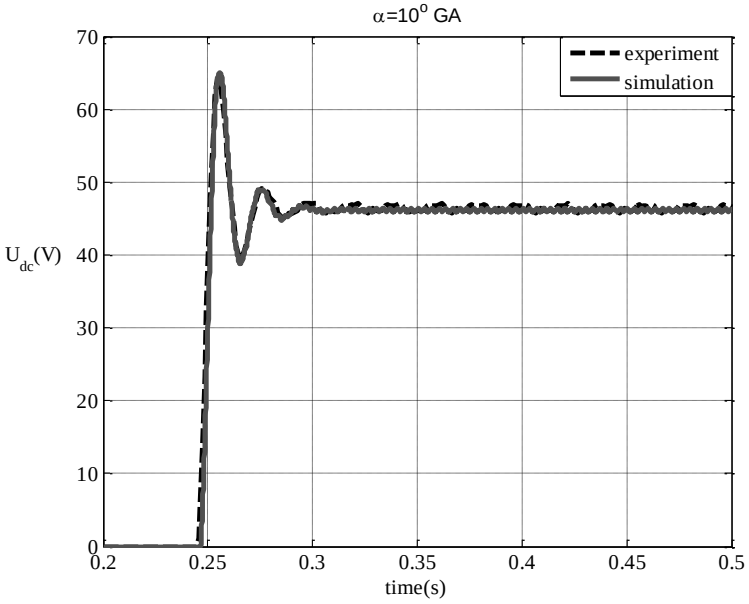

Figure 19. The Comparison Results to Validate the Identified Parameters from the GA Method (α = 10o)

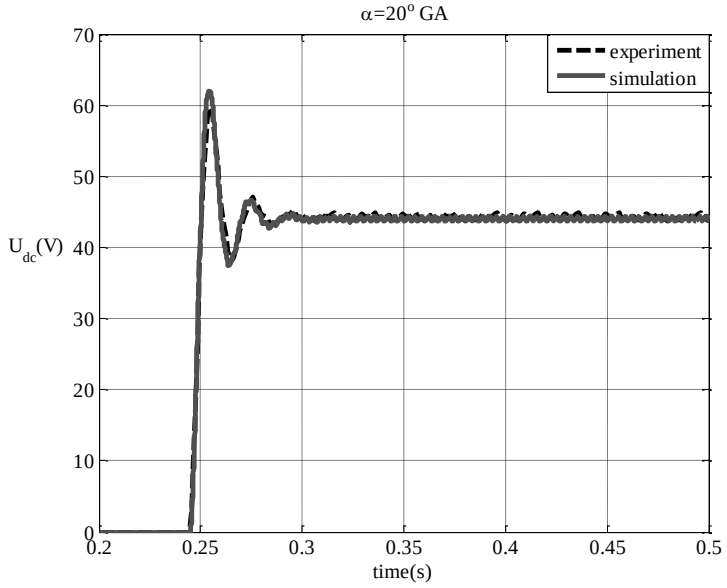

Figure 20. The Comparison Results to Validate the Identified Parameters from the GA Method (α = 20o)

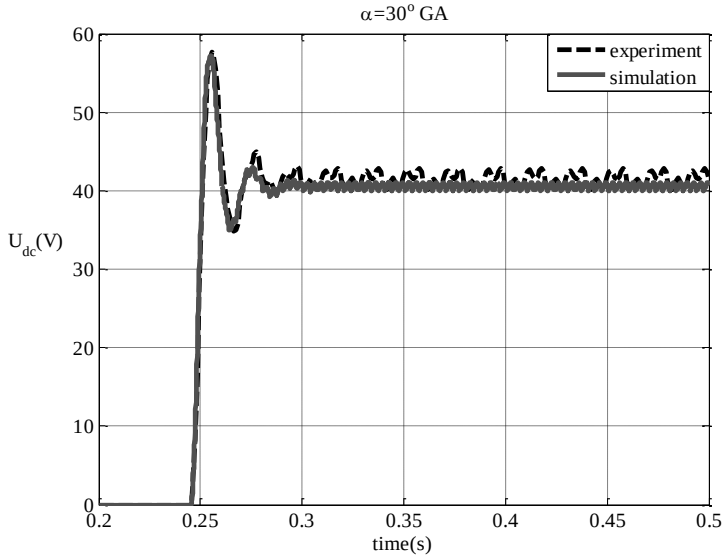

Figure 21. The Comparison Results to Validate the Identified Parameters from the GA Method (α = 30o)

From the results in Table I with Figure 14, Figure 21, the parameters identified from the ATS and GA methods are not the same. However, these parameters can provide the accurate response compared with the experimental results. Hence, the parameters from the proposed technique in the paper can be called *the equivalent parameter* in which it will be shown later that these different parameters from the different algorithms are suitable for the stability analysis.

After achieving the accurate parameters, the stability analysis due to the CPL of the power system in Figure 1 is illustrated in Section 6 in which the parameters determined from the ATS and GA techniques and measurement are used with the dynamic model to predict the unstable condition.

6. Stability Analysis

The stability analysis of the power system in Figure 1 is very important because of such system feeding CPLs. These loads can degrade the system stability. The stability analysis of the system in Fig. 1 needs the dynamic model in which the details of the model derivation can be founded in [20]. The work in [20] provides the equivalent circuit of the system in Figure 1. This equivalent circuit is suitable for the stability analysis due to a CPL as depicted in Figure 22.

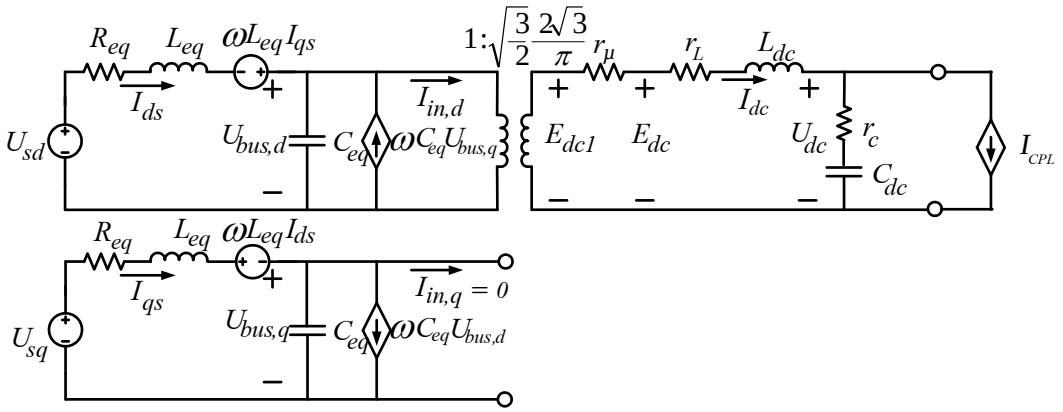

Figure 22. The Equivalent Circuit of the System in Figure 1 on DQ Frame

Applying the KVL and KCL into the circuit of Figure 22, the dynamic model of the system in Figure 1 can be expressed as given in (6).

$$\begin{aligned}
\dot{I}_{ds} &= -\frac{R_{eq}}{L_{eq}} I_{ds} + \omega I_{qs} - \frac{1}{L_{eq}} U_{bus,d} + \frac{1}{L_{eq}} U_{sd} \\
\dot{I}_{qs} &= -\omega I_{ds} - \frac{R_{eq}}{L_{eq}} I_{qs} - \frac{1}{L_{eq}} U_{bus,q} + \frac{1}{L_{eq}} U_{sq} \\
\dot{U}_{bus,d} &= \frac{1}{C_{eq}} I_{ds} + \omega U_{bus,q} - \sqrt{\frac{3}{2}} \frac{2\sqrt{3}}{\pi C_{eq}} I_{dc} \\
\dot{U}_{bus,q} &= -\omega U_{bus,d} + \frac{1}{C_{eq}} I_{qs} \\
\dot{I}_{dc} &= \sqrt{\frac{3}{2}} \frac{2\sqrt{3}}{\pi L_{dc}} U_{bus,d} - \frac{\left(r_\mu + r_L + r_c\right)}{L_{dc}} I_{dc} - \frac{1}{L_{dc}} U_{dc} - \frac{r_c P_{CPL}}{L_{dc} U_{dc}} \\
\dot{U}_{dc} &= \frac{1}{C_{dc}} I_{dc} - \frac{1}{C_{dc}} \frac{P_{CPL}}{U_{dc}}
\end{aligned} \tag{6}$$

To analyze the stability of the system by using the eigenvalue theorem, (6) is therefore linearized using the first order terms of the Taylor expansion so as to achieve a set of linear differential equations around an equilibrium point. After applying the linearization technique, (6) is then of the form in (7).

$$\begin{cases} \delta \dot{\mathbf{x}} = \mathbf{A}(\mathbf{x}_o, \mathbf{u}_o)\delta\mathbf{x} + \mathbf{B}(\mathbf{x}_o, \mathbf{u}_o)\delta\mathbf{u} \\ \delta\mathbf{y} = \mathbf{C}(\mathbf{x}_o, \mathbf{u}_o)\delta\mathbf{x} + \mathbf{D}(\mathbf{x}_o, \mathbf{u}_o)\delta\mathbf{u} \end{cases} \tag{7}$$

where

$$\delta\mathbf{x} = \begin{bmatrix} \delta I_{ds} & \delta I_{qs} & \delta U_{bus,d} & \delta U_{bus,q} & \delta I_{dc} & \delta U_{dc} \end{bmatrix}^T$$

$$\delta\mathbf{u} = \begin{bmatrix} \delta U_m & \delta P_{CPL} \end{bmatrix}^T$$

$$\delta\mathbf{y} = \begin{bmatrix} \delta U_{dc} \end{bmatrix}$$

$$\mathbf{A}(\mathbf{x_o},\mathbf{u_o})=\begin{bmatrix} -\frac{R_{eq}}{L_{eq}} & \omega & -\frac{1}{L_{eq}} & 0 & 0 & 0 \\ -\omega & -\frac{R_{eq}}{L_{eq}} & 0 & -\frac{1}{L_{eq}} & 0 & 0 \\ \frac{1}{C_{eq}} & 0 & 0 & \omega & \sqrt{\frac{3}{2}}\cdot\frac{2\sqrt{3}}{\pi C_{eq}} & 0 \\ 0 & \frac{1}{C_{eq}} & -\omega & 0 & 0 & 0 \\ 0 & 0 & \sqrt{\frac{3}{2}}\cdot\frac{2\sqrt{3}}{\pi L_{dc}} & 0 & -\frac{\left(r_\mu+r_L+r_c\right)}{L_{dc}} & -\left(\frac{1}{L_{dc}}+\frac{r_c P_{CPL}}{L_{dc}U_{dc}^2}\right) \\ 0 & 0 & 0 & 0 & \frac{1}{C_{dc}} & \frac{P_{CPL}}{C_{dc}U_{dc,o}^2} \end{bmatrix}_{6\times 6}$$

$$\mathbf{B}(\mathbf{x_o},\mathbf{u_o})=\begin{bmatrix} \sqrt{\frac{3}{2}}\cdot\frac{\cos(\lambda_o+\alpha)}{L_{eq}} & 0 \\ \sqrt{\frac{3}{2}}\cdot\frac{\sin(\lambda_o+\alpha)}{L_{eq}} & 0 \\ 0 & 0 \\ 0 & 0 \\ 0 & \frac{r_c}{L_{dc}U_{dc,0}} \\ 0 & -\frac{1}{C_{dc}U_{dc,o}} \end{bmatrix}_{6\times 2}$$

$$\mathbf{C}(\mathbf{x_o},\mathbf{u_o})=\begin{bmatrix}0 & 0 & 0 & 0 & 0 & 1\end{bmatrix}_{1\times 6} \qquad \mathbf{D}(\mathbf{x_o},\mathbf{u_o})=\begin{bmatrix}0 & 0\end{bmatrix}_{1\times 2}$$

According to linearized model in (7), the model needs to define $U_{dc,o}$ and λ_o. The details how to calculate these steady-state value and the model validation can be founded in [20]. The aim of this section is to show how to use the accurate parameters of the considered power system determined by the ATS and GA methods to predict the unstable point. The eigenvalues of the system with the given parameters of Table I are calculated from the Jacobian matrix when the P_{CPL} varies from 0 W to 500 W. The dominant eigenvalues calculated from the model in (7) with the system parameters from the ATS method (for α = 10^o) are shown in Figure 23.

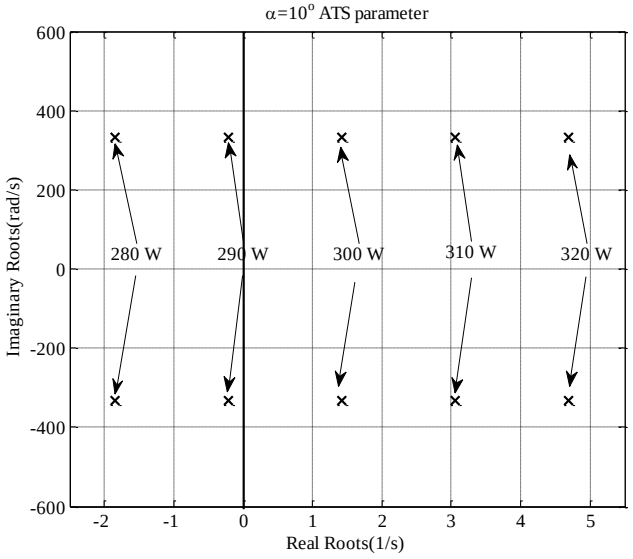

Figure 23. Eigenvalue Plot using the System Parameters Identified by ATS Method (for α = 10o)

Based on the eigenvalue theorem, it can be seen that the system becomes unstable when the P_{CPL} exceeds ~290 W. Figure 24 shows the time-domain simulations that support the theoretical results with instability occurring at P_{CPL} equal to 300 W. This is greater than 290

W for the unstable condition predicted from the theory. It can be seen from the results that the theoretical stability result can accurately predict the instability point of the system.

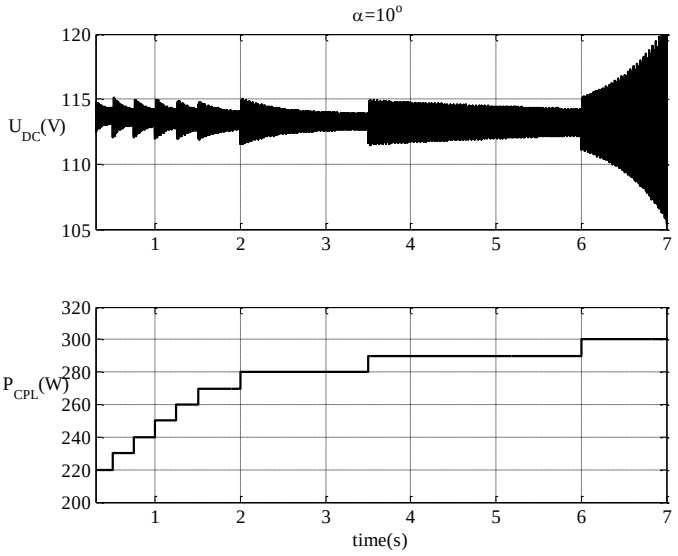

Figure 24. The Simulation Result for the Unstable Operation

As for GA method, the dominant eigenvalues calculated from the model in (7) with the system parameters from the GA method (for $\alpha = 10^{o}$) are shown in Figure 25.

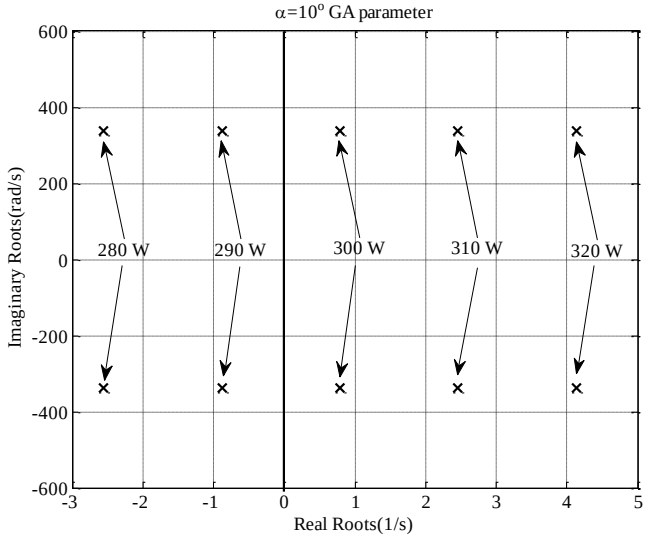

Figure 25. Eigenvalue Plot using the System Parameters Identified by GA Method (for α = 10o)

Interestingly, the different parameters identified from the ATS and GA methods can predict the identical unstable point. The unstable point is also confirmed by the simulation as shown in Figure 24 in which a good agreement between the theoretical (using both parameters from ATS and GA methods) and simulation results is obtained. For this point, it

can be summarized that the different parameters determined from the ATS and GA methods can provide the same *damping behavior* of the system in Figure 1. Therefore, the stability results when we use the dynamic model with the different parameters from ATS and GA methods can predict the same unstable point.

7. Conclusion

This paper presents how to determine the parameters of the DC-link filter and AC line elements of the AC-DC power system feeding the ideal CPL. The damping test system is firstly established for the system identification. The ATS and GA methods are co-operated with the averaging model and the experimental results of the damping test system to identify the system parameters. The results show that the accurate parameters can be achieved from the proposed technique. As for the stability analysis, the precise dynamic model cannot predict the unstable condition without the accurate system parameters. Therefore, the works of this paper show that the accurate parameters from the searching method are very useful and suitable for the stability studies of practical systems. The instability condition can be predicted from the DQ dynamic model with the resulting parameters in which the simulation result is used to validate the unstable operation. Moreover, the different parameters identified by the different techniques, here is the ATS and GA methods, can provide the identical unstable point. Hence, it can be said that the system identification by using the artificial technique cannot provide the unique solution. However, the different solutions can provide the unique unstable point. This is because the experimental results from the testing rig are used during the searching process to confirm that the parameters obtained from the searching method can describe the damping behavior of the practical system. The different parameters called the equivalent system parameters can be applied for the stability analysis with the accurate result.

Acknowledgements

This work was supported by Suranaree University of Technology (SUT) and the office of the Higher ducation Commission under NRU project of Thailand**.** The author would like to thank Assoc. Prof. Dr. Deacha Puangdownreong for providing the useful information of ATS algorithm.

References

[1]. R. D. Middlebrook, "Input Filter Consideration in Design and Application of Switching Regulators", **(1976)** October, Chicago, Illinois.
[2]. A. Emadi, B. Fahimi and M. Ehsani, "On the Concept of Negative Impedance Instability in the More Electric Aircraft Power Systems with Constant Power Loads", **(1999).**
[3]. C. Rivetta, G. A., Williamson and A. Emadi, "Constant Power Loads and Negative Impedance Instability in Sea and Undersea Vehicles", Statement of the Problem and Comprehensive Large-Signal Solution, **(2005)** July, Philadelphia, PA USA.
[4]. A. Emadi, A. Khaligh, C. H. Rivetta and G. A. Williamson, "Constant Power Loads and Negative Impedance Instability in Automotive Systems", Definition, Modeling, Stability, and Control of Power Electronic Converters and Motor Drives, vol. 4, no. 55, **(2006).**
[5]. A. Emadi, "Modeling and Analysis of Multiconverter DC Power Electronic Systems Using the Generalized State-Space Averaging Method", vol. 3, no. 51, **(2004).**
[6]. A. Emadi, Modeling of Power Electronic Loads in AC Distribution Systems Using the Genearlized State-Space Averaging Method, vol. 5, no. 51, **(2004)** October.
[7]. L. Han, J. Wang and D. Howe, "State-space average modelling of 6- and 12-pulse diode rectifiers", The 12th European Conf. on Power Elect. and Appl., **(2007)** September, Aalborg, Denmark.

[8]. A. Baghramian, and A.J. Forsyth, "Averaged-Value Models of Twelve-Pulse Rectifiers for Aerospace Applications", Power Electronics, Machines, and Drives (PEMD 2004), **(2004)** March-April, University of Edinburgh, UK.
[9]. S. D. Sudhoff and O. Wasynczuk, Analysis and Average-Value Modeling of Line-Commutated Converter-Synchronous Machine Systems, vol. 1, no. 8, **(1993).**
[10]. C. T. Rim, D. Y. Hu and G. H. Cho, Transformers as Equivalent Circuits for Switches: General Proofs and D-Q Transformation-Based Analyses, vol. 4, no. 26, **(1990).**
[11]. C. T. Rim, N. S. Choi, G. C. Cho and G. H. Cho, A Complete DC and AC Analysis of Three-Phase Controlled-Current PWM Rectifier Using CircuitD-Q Transformation, vol. 4, no. 9, **(1994).**
[12]. S. B. Han, N. S. Choi, C. T. Rim and G. H. Cho, Modeling and Analysis of Static and Dynamic Characteristics for Buck-Type Three-Phase PWM Rectifier by Circuit DQ Transformation, vol. 2, no. 13, **(1998).**
[13]. K-N. Areerak, S. V. Bozhko, G. M. Asher and D. W. P. Thomas, "Stability Analysis and Modelling of AC-DC System with Mixed Load Using DQ-Transformation Method", IEEE International Symposium on Industrial Electronics (ISIE08), **(2008)** June 29- July 2, Cambridge, UK.
[14]. K-N. Areerak, S. V. Bozhko, G. M. Asher and D. W. P. Thomas, "DQ-Transformation Approach for Modelling and Stability Analysis of AC-DC Power System with Controlled PWM Rectifier and Constant Power Loads", 13th International Power Electronics and Motion Control Conference (EPE-PEMC 2008), **(2008)** September 1-3, Poznan, Poland.
[15]. K-N. Areerak, S. Bozhko, G. Asher, L. de Lillo, A. Watson, T. Wu and D. W. P. Thomas, "The Stability Analysis of AC-DC Systems including Actuator Dynamics for Aircraft Power Systems", 13th European Conference on Power Electronics and Applications (EPE 2009),**(2009)** September 8-10, Barcelona, Spain.
[16]. D. Puangdownreong, K-N. Areerak, A. Srikaew, S. Sujijorn and P. Totarong, "System Identification via Adative Tabu Search", In Proceedings IEEE International Conference on Industrial Technology (ICIT02), **(2002)**.
[17]. D. Puangdownreong, K-N. Areerak, K-L. Areerak, T. Kulworawanichpong and S. Sujitjorn, "Application of adaptive tabu search to system identification", IASTED International Conference on Modelling, Identification, and Control (MIC2005), **(2005)** February16-18, Innsbruck, Austria.
[18]. T. Kulworawanichpong, K-L. Areerak, K-N. Areerak, P. Pao-la-or, D. Puangdownreong and S. Sujitjorn, "Dynamic parameter identification of induction motors using intelligent search techniques", IASTED International Conference on Modelling, Identification, and Control (MIC2005), **(2005)** February 16-18, Innsbruck, Austria.
[19]. T. Kulworawanichpong, K-L. Areerak, K-N. Areerak, and S. Sujitjorn, "Harmonic Identification for Active Power Filters via Adaptive Tabu Search Method", LNCS (Lecture Notes in Computer Science), Springer-Verlag Heidelberg, vol. 3215, **(2004)**, pp. 687-694.
[20]. K. Chaijarurnudomrung, K-N. Areerak and K-L. Areerak, "Modeling of Three-phase Controlled Rectifier using a DQ method", 2010 International Conference on Advances in Energy Engineering (ICAEE 2010), **(2010)**.

